Ti *K* Pre-Edge in $SrTiO_3$ under Pressure: Experiments and Full-Potential First-Principles Calculations

D. Cabaret*, B. Couzinet*, A.-M. Flank†, J.-P. Itié†, P. Lagarde† and A. Polian*

*Institut de Minéralogie et de Physique des Milieux Condensés, CNRS UMR7590, Université Pierre et Marie Curie, Paris 6, 140 rue de Lourmel, F-75015 Paris, France

†Synchrotron SOLEIL, L'orme des merisiers, Saint-Aubin - BP 48, F-91192 Gif-sur-Yvette cedex, France

Abstract. Strontium titanate exhibits two phase transitions at 5 GPa and 14 GPa. We use X-ray absorption Ti *K* pre-edge structure as a probe of the local atomic structure of $SrTiO_3$ under pressure. The pre-edge is characterized by four main features labeled A, B, C_1 and C_2. Above 5 GPa, the intensity of peak B is decreased while that of the double feature C_1-C_2 is increased. By increasing the pressure above 14 GPa, peak A shifts towards lower energy and of peak C_1 towards higher energy. While the first phase transformation is known to be a transition from the cubic phase to a tetragonal one, the second phase transformation leads to a crystal structure not yet identified. To analyze these spectral modifications, full-potential first principles simulations of Ti *K* pre-edge are performed. The calculations provide a good agreement with experiments and permits the identification of the four features in terms of orbital hybridization. Trial crystal structures are proposed in order to account for the pre-edge modifications observed under pressure.

Keywords: strontium titanate, perovskite, pre-edge, Ti K-edge, ab initio, pseudopotential
PACS: 61.10.Ht,78.70.Dm,81.40.Vw,71.20.-b,77.84.-s

INTRODUCTION

Although structural phase transitions in the solid state have been extensively studied in the last decades, the case of ferroelectric titanate perovskite is still of great interest in condensed matter physics. For example, Stern [1] recently explained the respective role of displacive and order-disorder components in the cubic-tetragonal phase transition of $BaTiO_3$. More recently, Ti *K*-edge X-ray absorption near-edge structure (XANES) measurements under pressure have revealed the disappearance of the local rhombohedral distortion in $BaTiO_3$ [2].

This paper is devoted to the pressure induced phase transitions of $SrTiO_3$ that are investigated by X-ray absorption spectroscopy in the Ti *K* pre-edge range. Indeed this region is a probe of the local Ti environment since it involves electronic transitions into unfilled Ti *d* levels [3]. The interpretation of the experimental spectra is carried out with the help of non "muffin-tin" first-principles calculations using the method described in [4, 5].

METHODS

Experiments are performed at the LUCIA beamline of SLS (Swiss Light Source) at the Ti *K* edge in a membrane diamond anvill cell. A Si (111) double crystal monochromator is used and the detection is done in transmission mode with a Si diode. XANES measurements are carried out on $SrTiO_3$ powder sample up to 30 GPa. Further experimental details are given in [6].

XANES calculations are performed using a plane-wave electronic structure code[1], based on density functional theory (DFT) in the local density approximation (LDA), in which has been recently implemented the calculation of X-ray absorption spectra in electric dipole and quadrupole approximations [4, 5]. The method uses Troullier-Martins norm-conserving pseudopotentials, periodic boundary conditions and compute the absorption cross section as a continued fraction in both electric dipole (E_1) and quadrupole (E_2) approximations. In all the calculations the plane-wave expansion is limited by a cut-off of 80 Ry and the continued fraction is computed with a broadening parameter γ=0.68 eV. For supercell calculations, the self-consistent potential is determined on one *k*-point, while the cross section computations require $3\times3\times3$ *k*-point grids.

RESULTS AND DISCUSSION

Figure 1 presents three Ti *K* pre-edge experimental spectra recorded at 1, 11.7 and 30 GPa, showing the effects of two phase transitions of $SrTiO_3$ occurring at 5 and 14 GPa. The three pre-edge exhibits four main peaks labeled A, B, C_1 and C_2. The first phase transformation is characterized by an intensity decrease and an energy

[1] PARATEC (PARAllel Total Energy Code) by B. Pfrommer, D. Raczkowski, A. Canning, S.G. Louie, Lawrence Berkeley National Laboratory.

shift (+0.4 eV) of peak B, and by an intensity increase of peaks C_1 and C_2. The second transition shows energy shifts of peak A (-0.5 eV) and of peak C_1 (+0.4 eV). Simulations are needed to analyze these modifications.

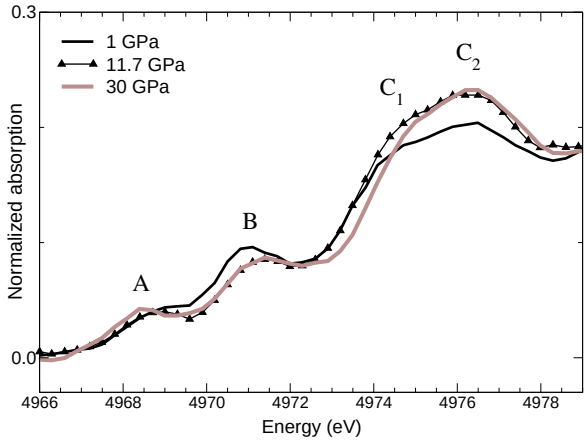

FIGURE 1. Experimental Ti *K* pre-edge recorded in $SrTiO_3$ at 1 GPa, 11.7 GPa and 30 GPa

First we focus on the cubic phase to understand the origin of the four pre-edge features. Second, distorted perovskite structures are tested in order to reproduce the pressure induced changes observed in pre-edge region.

For the ambient conditions phase, the calculations are performed in the $Pm\bar{3}m$ cubic structure where Ti atoms occupy O_h symmetry site [7]. Figure 2 displays the theoretical pre-edge spectra calculated with or without the 1*s* core-hole on the Ti absorbing atom. The core-hole is taken into account within a $3\times3\times3$ supercell (135 atoms), in agreement with Ref. [8]. Figure 2 also shows the E_2 contributions separately. The presence of the 1*s*

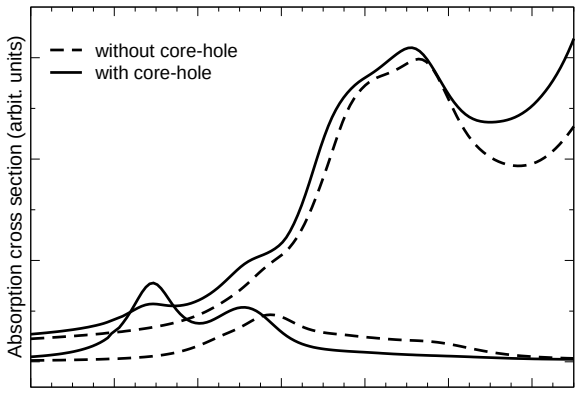

FIGURE 2. Calculated Ti *K*-pre-edge with and without core-hole for the cubic ambient phase The total cross section is labeled E_1+E_2, and the isotropic E_2 contribution is multiplied by a factor 4.

core-hole essentially produces a shift of the E_2 transitions towards lower energy, as in rutile [9], explaining the origin of peaks A and B. This energy shift is not large enough. This discrepancy with experiment is due to DFT-LDA which is limited in the modelling of electron-hole interaction [10]. The too small theoretical intensity of B feature is also in disagreement with experiment.

Peaks C_1 and C_2 result from E_1 transitions, and are very slightly affected by the core-hole (Figs. 2 and 3). In figure 3 we compare E_1 and E_2 cross sections with partial density of empty states (pDOS) performed without core hole and using the same code. The cross sections

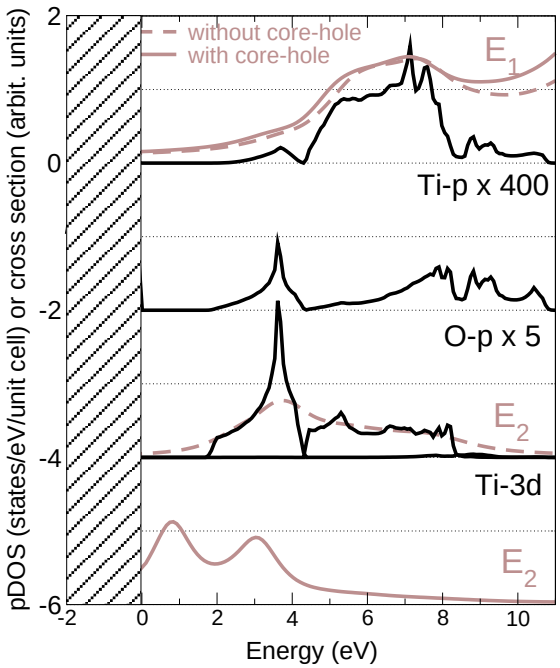

FIGURE 3. Theoretical E_1 and E_2 spectra calculated compared with ground state pDOS calculations

and the corresponding pDOS have very similar shapes, i.e. the energy-dependence of the radial transition matrix elements is negligible within pseudopotential framework. Figure 3 then shows that C_1 and C_2 features are due to $1s \rightarrow p$ transitions and that the empty *p* states of Ti absorbing atom are hybridized with the $3d$-e_g states of neighboring Ti via O-*p* states. Peak *B* has a very weak E_1 contribution resulting from the hybridization of *p* states of absorbing Ti and $3d$-t_{2g} states of neighboring Ti. However this contribution is not large enough to reproduce the experimental strength of peak B. If Ti was not in a centrosymmetric site, the mixing between *p* and $3d$-e_g states of absorbing Ti atom would be allowed and then increase the intensity of peak B. This is illustrated in figure 4 that exhibits theoretical spectra obtained with Ti displaced along the [111] direction. According to this figure, the Ti displacement from the centrosymmetric site should be around 0.1 Å in order to explain the experimental intensity of feature B. Complementary studies are needed to

determine if this off-center disorder could be either static or dynamic.

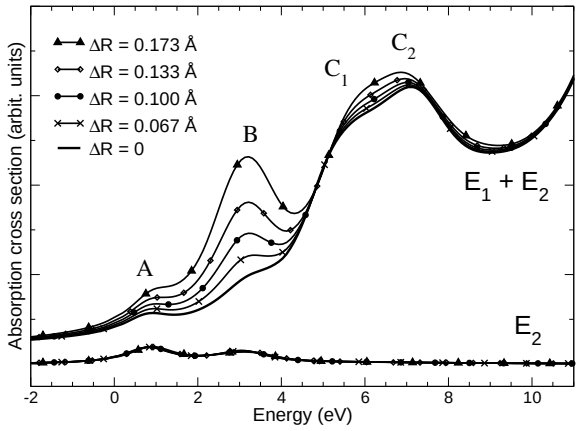

FIGURE 4. Theoretical spectra with various off-site Ti positions. ΔR is the shift of Ti along the [111] direction

The second pressure induced phase transition is known to be a cubic to tetragonal one. We use the tetragonal crystal structure of the low-temperature phase (space group $I4/mcm$) given in [11], where the TiO_6 octahedra are tilted (tilt angle ϕ=1.12°). Calculations are performed using a $2\times2\times2$ supercell. Unfortunately this structure does not explain the intensity increase of C_1 and C_2, even if B strentgh is decreased and C_1 slightly shifted towards higher energy (see figure 5). Greater tilt angles do not improve the agreement with experiment. For

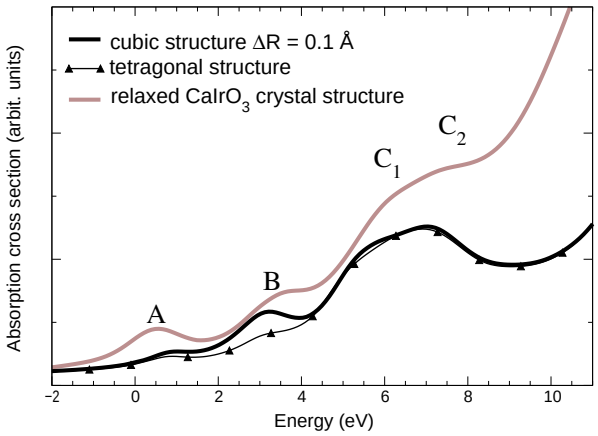

FIGURE 5. Theoretical Ti K pre-edge for cubic structure with off-center Ti, for low-temperature tetragonal structure and for $CaIrO_3$ relaxed structure.

the high-pressure phase, the $CaIrO_3$ orthorhombic perovskite structure with space group $Cmcm$ [12] is considered, mainly because the TiO_6 octahedron presents two kinds of Ti-O distances, that are supposed to be responsible for the shifts of the two E_2 peaks. A $3\times1\times1$ supercell is built after a total energy minimization of the $SrTiO_3$ unit cell with the $CaIrO_3$ geometry. The corresponding cross section shows too important spectral changes but their trends are in agreement with the modifications observed experimentally (see figure 5). In particular, peaks A and C_1 are oppositely shifted and the intensity of C_1 and C_2 are increased.

CONCLUSION

Thanks to first-principles full-potential calculations, we give an interpretation of the Ti K pre-edge features in $SrTiO_3$. In the cubic phase, our results are in agreement with [8, 13]. We find that E_2 transitions cannot explain the whole intensity of feature B: E_1 transitions should be present, that implies a Ti off-center disordered position. The tilt of the octahedron in the low-temperature tetragonal phase does not explain all the modifications observed in the 11.7 GPa experimental spectrum. On the other hand, considering distorted octahedron with 2 Ti-O distances, as in $CaIrO_3$, leads to trends in agreement with experiments.

We acknowledge the computational support of IDRIS in Orsay, France (project 1202).

REFERENCES

1. E. Stern, *Phys. Rev. Lett.* **93**, 037601 (2004).
2. J. P. Itié, B. Couzinet, A. Polian, A.-M. Flank, and P. Lagarde, *Europhys. Lett.* **74**, 706–711 (2006).
3. B. Ravel, E. Stern, R. Vedrinskii, and V. Kraizman, *Ferroelectrics* **206-207**, 407 (1998).
4. M. Taillefumier, D. Cabaret, A.-M. Flank, and F. Mauri, *Phys. Rev. B* **66**, 195107 (2002).
5. D. Cabaret, E. Gaudry, M. Taillefumier, P. Sainctavit, and F. Mauri, *Physica Scripta, Proc. XAFS-12 conference* **T115**, 131–133 (2005).
6. J. P. Itié, B. Couzinet, A.-M. Flank, P. Lagarde, and A. Polian, *Poster number WE-PO.49 and these proceedings* (2006).
7. Y. A. Abramov, V. G. Tsirelson, V. E. Zavodnik, S. A. Ivanov, I. D. Ivanov, and I. D. Brown, *Acta Cryst.* **B51**, 942–951 (1995).
8. T. Yamamoto, T. Mizoguchi, and I. Tanaka, *Phys. Rev. B* **71**, 245113 (2005).
9. Y. Joly, D. Cabaret, H. Renevier, and C. R. Natoli, *Phys. Rev. Lett.* **82**, 2398–2401 (1999).
10. E. Gaudry, D. Cabaret, P. Sainctavit, C. Brouder, F. Mauri, J. Goulon, and A. Rogalev, *J. Phys.: Condens. Matter* **17**, 5467–5480 (2005).
11. K. Tsuda, and M. Tanaka, *Acta Cryst. A* **51**, 7–19 (1995).
12. F. Rodi, and D. Babel, *Z. Anorg. Allg. Chem.* **336**, 17–23 (1965).
13. R. V. Vedrinskii, V. L. Kraizman, A. A. Novakovich, P. V. Demekhin, and S. V. Urazhdin, *J. Phys.: Condens. Matter* **10**, 9561–9580 (1998).